Acta Crystallographica Section F
Structural Biology Communications
ISSN 2053-230X

Crystallization and preliminary X-ray crystallographic studies of dehydroascorbate reductase (DHAR) from *Oryza sativa* L. *japonica*

Hackwon Do,[a,b]‡ Il-Sup Kim,[c]‡ Young-Saeng Kim,[c] Sun-Young Shin,[c] Jin-Ju Kim,[c] Ji-Eun Mok,[c] Seong-Im Park,[c] Ah Ram Wi,[a] Hyun Park,[a,b] Han-Woo Kim,[a]* Ho-Sung Yoon[c]* and Jun Hyuck Lee[a,b]*

[a]Division of Polar Life Sciences, Korea Polar Research Institute, Incheon 406-840, Republic of Korea, [b]Department of Polar Sciences, Korea University of Science and Technology, Incheon 406-840, Republic of Korea, and [c]Department of Biology, Kyungpook National University, Daegu 702-701, Republic of Korea

‡ HD and I-SK contributed equally to this work.

Correspondence e-mail: hwkim@kopri.re.kr, hyoon@knu.ac.kr, junhyucklee@kopri.re.kr

Received 25 February 2014
Accepted 22 April 2014

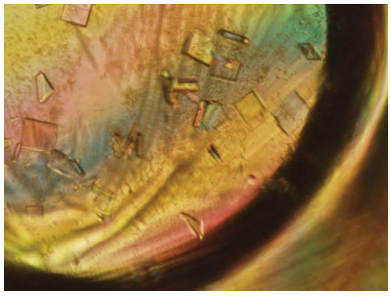

Dehydroascorbate reductase from *Oryza sativa* L. *japonica* (OsDHAR), a key enzyme in the regeneration of vitamin C, maintains reduced pools of ascorbic acid to detoxify reactive oxygen species. In previous studies, the overexpression of OsDHAR in transgenic rice increased grain yield and biomass as well as the amount of ascorbate, suggesting that ascorbate levels are directly associated with crop production in rice. Hence, it has been speculated that the increased level of antioxidants generated by OsDHAR protects rice from oxidative damage and increases the yield of rice grains. However, the crystal structure and detailed mechanisms of this important enzyme need to be further elucidated. In this study, recombinant OsDHAR protein was purified and crystallized using the sitting-drop vapour-diffusion method at pH 8.0 and 298 K. Plate-shaped crystals were obtained using 0.15 *M* potassium bromide, 30%(*w*/*v*) PEG MME 2000 as a precipitant, and the crystals diffracted to a resolution of 1.9 Å on beamline 5C at the Pohang Accelerator Laboratory. The X-ray diffraction data indicated that the crystal contained one OsDHAR molecule in the asymmetric unit and belonged to space group $P2_1$ with unit-cell parameters a = 47.03, b = 48.38, c = 51.83 Å, β = 107.41°.

1. Introduction

Ascorbic acid (ascorbate or vitamin C) is a major reducing agent in the antioxidation process against reactive oxygen species (ROS) that result from various environmental stresses (high salinity, cold temperature, drought and UV light) and are present in millimolar concentrations in plant cells (Arrigoni, 1994; Gallie, 2013). ROS can cause oxidative damage to proteins, nucleic acids and lipid membranes, leading to major agricultural problems resulting in reduced crop yields. Thus, understanding the synthesis and maintenance of vitamin C in plant sources may possibly facilitate the development of nutrient-rich foods using biotechnological methods (Tommasi *et al.*, 2001; Yin *et al.*, 2010). During the antioxidation process, ascorbic acid is oxidized to monodehydroascorbate (MDHA) by ascorbate peroxidase (APX) and hydrogen peroxide is reduced to H_2O; the MDHA produced spontaneously disproportionates into dehydroascorbate (DHA). As a result, plants need to regenerate reduced ascorbic acid again, which involves recycling oxidized ascorbic acid into a reduced form. Plants have two key enzymes for recycling oxidized ascorbic acid. DHA reductase (DHAR; EC 1.8.5.1) catalyzes the re-reduction of DHA to ascorbic acid using glutathione as a reducing agent, and monodehydroascorbate reductase (MDHAR) reduces MDHA to ascorbic acid using NAD(P)H as a reductant (Arrigoni, 1994; Chen *et al.*, 2003; Chen & Gallie, 2006; Gallie, 2013).

The rapid reduction of DHA to ascorbic acid by DHAR is important for maintaining the intracellular redox state (Ushimaru *et al.*, 2006). We recently demonstrated that overexpression of DHAR in transgenic rice induced a significant increase in ascorbic acid levels and in crop production (Kim *et al.*, 2013; Shin *et al.*, 2013). Thus, ascorbic acid levels are closely associated with grain yield. However, little is known about the enzymatic mechanism and the three-dimensional structure of DHAR. The most similar homologous protein known is most likely to be the human chloride ion channel protein 1 (CLIC1; PDB entry 1k0m; Harrop *et al.*, 2001), which shares 32% sequence identity with OsDHAR. Unlike DHAR, CLIC

proteins exist as soluble globular proteins in the cytosol, but they can form ion channels in plasma membranes (Cromer *et al.*, 2002). In previous electrophysiology studies, chloride-selective channel activity was observed in CLIC1-transfected Chinese hamster ovary cells (Warton *et al.*, 2002) as well as in phospholipid vesicles mixed with CLIC1 (Tulk *et al.*, 2002). In addition, the structural change of CLIC1 from the soluble monomer form to the membrane-inserted dimer form has been proposed as a means of regulating channel activity and subcellular distribution (Cromer *et al.*, 2002). It is now known that an intermolecular disulfide-bond formation (Cys24–Cys59) in monomeric CLIC1 protein induces a conformational change to a new dimer structure, thereby exposing a large hydrophobic surface for membrane insertion (Littler *et al.*, 2004).

In this study, dehydroascorbate reductase from *Oryza sativa* L. *japonica* (OsDHAR) was cloned, overexpressed using an *Escherichia coli* expression system and purified (UniProtKB code Q65XA0; 213 amino-acid residues). We also successfully crystallized and collected a complete native X-ray diffraction data set for OsDHAR. We believe that this first DHAR crystal structure will be valuable for elucidating the mechanism of this enzyme.

2. Materials and methods

2.1. Cloning, expression, and purification of OsDHAR

The construction of a full-length cDNA encoding OsDHAR has been described previously (Shin *et al.*, 2008; Kim *et al.*, 2013). Briefly,

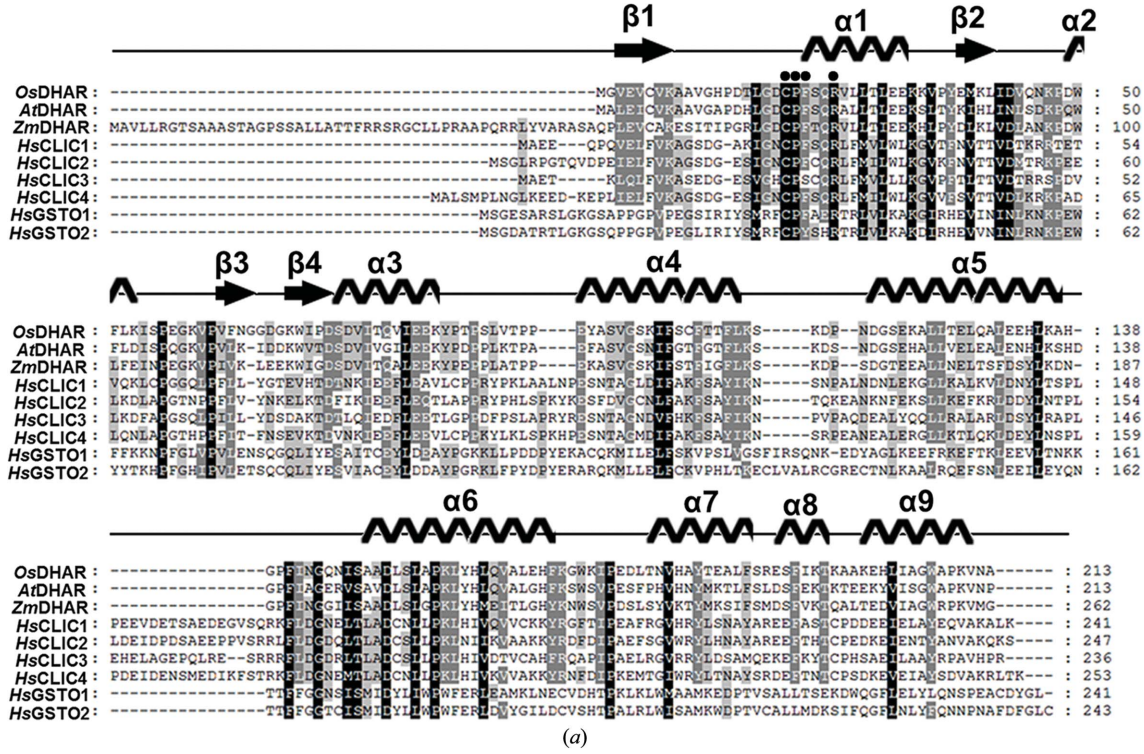

(*a*)

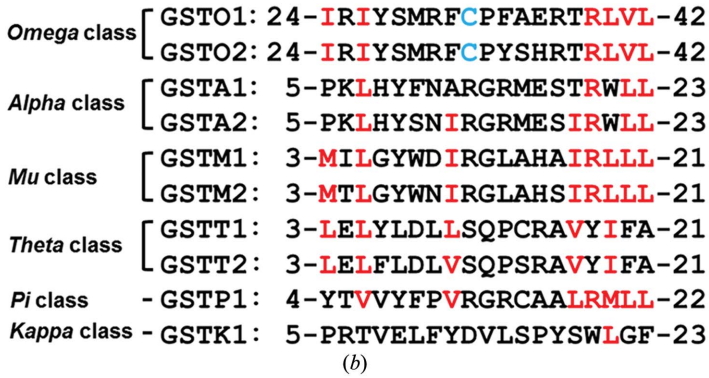

(*b*)

Figure 1
Sequence alignments of OsDHAR, CLICs and GSTs. (*a*) The following amino-acid sequences were aligned using *ClustalX* (Thompson *et al.*, 1997): OsDHAR, *Oryza sativa* (UniProtKB code Q65XA0); AtDHAR, *Arabidopsis thaliana* (UniProtKB code Q9FWR4); ZmDHAR, *Zea mays* (UniProtKB code B6U098); HsCLIC1, *Homo sapiens* (UniProtKB code O00299); HsCLIC2, *H. sapiens* (UniProtKB code O15247); HsCLIC3, *H. sapiens* (UniProtKB code O95833); HsCLIC4, *H. sapiens* (UniProtKB code Q9Y696); HsGST1, *H. sapiens* (UniProtKB code P78417); and HsGST2, *H. sapiens* (UniProtKB code Q9H4Y5). The highly conserved residues are shaded in black. The secondary-structural elements of OsDHAR were predicted using the *Phyre* server (Kelley & Sternberg, 2009) and are shown above the alignments. Notably, OsDHAR has a conserved catalytic cysteine residue and GSH-binding residues, which are indicated by a filled circle (Harrop *et al.*, 2001). (*b*) Sequence alignments of various types of GSTs from *H. sapiens*, including GSTO1 (UniProtKB code P78417), GSTO2 (UniProtKB code Q9H4Y5), GSTA1 (UniProtKB code P08263), GSTA2 (UniProtKB code P09210), GSTM1 (UniProtKB code P09488), GSTM2 (UniProtKB code P28161), GSTT1 (UniProtKB code P30711), GSTT2 (UniProtKB code P0CG29), GSTP1 (UniProtKB code P09211) and GSTK1 (UniProtKB code Q9Y2Q3). The amino-acid sequences around the conserved catalytic cysteine residue (blue) in omega-class GSTs are shown here. Note that omega-class GSTs have a conserved cysteine residue (blue) for GSH binding, whereas the cysteine residue is absent in other classes of GSTs. Strongly conserved residues are not seen here; moderately conserved residues are coloured red.

Table 1
Data-collection statistics.

Values in parentheses are for the last resolution shell.

X-ray source	5C, PAL
Space group	$P2_1$
Unit-cell parameters (Å, °)	a = 47.03, b = 48.38, c = 51.83, β = 107.41
Wavelength (Å)	0.97955
No. of frames	360
Oscillation angle (°)	1
Resolution range (Å)	34.58–1.90 (2.00–1.90)
No. of observed reflections	116285 (17553)
No. of unique reflections	17083 (2483)
Completeness (%)	97.0 (97.1)
Multiplicity	6.8 (7.1)
$R_{\rm merge}$†	0.121 (0.294)
Average $I/\sigma(I)$	12.3 (7.0)

† $R_{\rm merge} = \sum_{hkl}\sum_i |I_i(hkl) - \langle I(hkl)\rangle| / \sum_{hkl}\sum_i I_i(hkl)$, where $I_i(hkl)$ is the value of the ith intensity measurement and $\langle I(hkl)\rangle$ is the mean value of all measurements of $I(hkl)$.

total RNA was isolated from the leaves of *O. sativa* using an RNeasy Plant Mini Kit (Qiagen, Hilden, Germany). The cDNA probe was synthesized using an RT-PCR Premix Kit (Bioneer, Daejeon, Republic of Korea) according to the manufacturer's instructions. The OsDHAR gene (UniProtKB code Q65XA0; NCBI accession No. AY074786.1) was amplified from cDNA by PCR using *ExTaq* polymerase (TaKaRa Bio Inc., Tokyo, Japan) with 5′-TCG CCG **CCA TGG** GCG TGG AGG TGT GCG-3′and 5′-CCA AGC AAG **GGA TCC** TGC AGG CTG CAT CTC CAT TAT TC-3′ as the sense and antisense primers, respectively. The bold sequences indicate the *Nco*I and *Bam*HI restriction-enzyme sites, respectively. The PCR reaction conditions were as follows: initial denaturation at 367 K for 3 min, 30 cycles of 367 K for 30 s, 327 K for 30 s and 345 K for 1.5 min, and final extension at 345 K for 7 min. The PCR product was purified using a Gel Extraction Kit (Nucleogen, Siheung, Republic of Korea) and then inserted into the TOPO-TA cloning vector (Invitrogen, Carlsbad, USA). The cloned plasmid was sequenced using the M13 primer set to confirm that no PCR-induced mutations had been introduced, after which it was digested with the *Nco*I and *Bam*HI restriction enzymes.

The digested plasmid DNA fragment was ligated into the *E. coli* expression vector pKM260 (Euroscarf, Frankfurt, Germany) and the resulting plasmid was named pKM260::OsDHAR. *E. coli* NiCo21 (DE3) cells were transformed with the pKM260::OsDHAR plasmid by the $CaCl_2$-mediated method (Shin *et al.*, 2008). Positive transformants were grown on Luria–Bertani (LB) agar plates supplemented with 50 µg ml^{-1} ampicillin for 24 h at 310 K. The strains containing the transformed plasmid (pKM260::OsDHAR) were used for protein expression. The transformed *E. coli* cells were grown in LB broth medium (6 l culture) containing 50 µg ml^{-1} ampicillin at 310 K until the optical density at 600 nm approached 0.4, and protein expression was then induced by the addition of 0.2 m*M* isopropyl β-D-1-thiogalactopyranoside (IPTG). The cells were then allowed to grow at 295 K for 18 h. The cell pellet was harvested by centrifugation at 4000*g* for 20 min and resuspended in cold lysis buffer (50 m*M* sodium phosphate pH 8.0, 300 m*M* NaCl, 5 m*M* imidazole) containing 0.2 mg ml^{-1} lysozyme and 0.5 m*M* phenylmethylsulfonyl fluoride (PMSF) and EDTA-free protease-inhibitor cocktail (PIC; Sigma, St Louis, USA). After incubation for 20 min on ice, the cells were disrupted by ultrasonication with short pulses (10 s) with pauses (10 s) for 1 h (Sonic Dismembrator 550; Fisher Scientific Inc., Pittsburgh, USA) on ice and the cell debris was removed by centrifugation at 10 000*g* for 30 min.

The cleared supernatant was poured into a gravity-flow column pre-packed with Ni–NTA resin (Qiagen, Hilden, Germany). The hexahistidine-tag-fused OsDHAR protein in the supernatant was bound to Ni–NTA resin and unbound protein was washed away with ten column volumes of wash buffer (50 m*M* sodium phosphate pH 8.0, 300 m*M* NaCl, 20 m*M* imidazole). OsDHAR protein was eluted with elution buffer (50 m*M* sodium phosphate pH 8.0, 300 m*M* NaCl, 250 m*M* imidazole). Desalting and concentration of OsDHAR protein using cold 20 m*M* Tris–HCl pH 8.0 and PIC was performed by Amicon Ultra Centrifugal Filters (Ultracel-10K; Millipore, Darmstadt, Germany) according to the manufacturer's instructions. The resulting protein was concentrated to 17.0 mg ml^{-1} for crystallization trials. Protein concentrations were spectrophotometrically determined using Protein Dye Reagent (Bio-Rad, Hercules, USA). The final recombinant OsDHAR contained an extra 17 amino acids (M**HHHHHH**ASENLYFQGA), including the hexahistidine tag (bold), at the N-terminus and the calculated molecular weight from the coding sequence was 25 605 Da.

2.2. Analytical size-exclusion chromatography

Analytical size-exclusion chromatography (SEC) was performed using a TSK gel G2000SWXL column (7.8 × 300 mm; Tosoh Co., Tokyo, Japan) connected to a YL9100 HPLC system controlled by the *YL-Clarity* software (available from the YL instrument website, http://www.younglin.com). The column was equilibrated in 20 m*M* sodium phosphate buffer pH 8, 150 m*M* NaCl at a flow rate of 1 ml min^{-1} at room temperature. The column was calibrated with the following set of globular protein standards (MWGF70-1KT; Sigma, St Louis, USA): albumin (66 kDa, V_e = 6.50 ml), carbonic anhydrase (29 kDa, V_e = 8.31 ml), cytochrome *c* (12.4 kDa, V_e = 10.70 ml) and aprotinin (6.5 kDa, V_e = 14.09 ml). The void volume was estimated based on the elution volume of Blue Dextran (2000 kDa, V_e = 5.37 ml).

2.3. Crystallization and data collection of OsDHAR

Initial crystallization screening was performed by the sitting-drop vapour-diffusion method using the following commercially available screening kits: the MCSG-1–4 series (Microlytic, Burlington, USA), the Wizard Classic I–IV series (Emerald Bio, Seattle, USA) and The Classics and Classics II Suites (Qiagen, Hilden, Germany) screens. Crystallization drops consisting of 0.8 µl protein solution (17.0 mg ml^{-1}) and 0.8 µl crystallization solution were equilibrated against 80 µl reservoir solution at 298 K. After 2 d, initial microcrystals appeared from MCSG-1 condition No. 8 [0.1 *M* Tris–HCl pH 7.0, 20%(*w*/*v*) PEG MME 2000], MCSG-2 condition No. 2 [0.15 *M* potassium bromide, 30%(*w*/*v*) PEG MME 2000], MCSG-2 condition No. 71 [0.2 *M* sodium tartrate dibasic, 20%(*w*/*v*) PEG 3350] and Wizard Classic III condition No. 5 [0.2 *M* ammonium chloride, 20%(*w*/*v*) PEG 3350].

These conditions were further optimized by varying the amount of precipitant and protein solutions. From these results, the best crystals of OsDHAR were obtained in 0.15 *M* potassium bromide, 30%(*w*/*v*) PEG MME 2000 at 298 K using the sitting-drop vapour-diffusion method in 24-well plates. The drop consisted of 1 µl protein solution and 2 µl reservoir solution and was equilibrated against 0.3 ml reservoir solution. Crystals of OsDHAR appeared within 1–2 d and grew in 3 d to maximum dimensions of 0.1 × 0.1 × 0.05 mm. The crystal was soaked and passed through Paratone-N oil as a cryoprotectant (Hampton Research, Aliso Viejo, USA) for 1 min.

Before collecting the X-ray diffraction data, the crystal was directly flash-cooled in a 100 K nitrogen-gas stream. Diffraction data were

collected on beamline 5C of the Pohang Accelerator Laboratory (PAL; Pohang, Republic of Korea) with 1° oscillations with 1 s exposure time over a total of 360° at a wavelength of 0.97955 Å using an ADSC Q315r CCD detector. The data set was indexed and integrated using *iMosflm* (Battye *et al.*, 2011). Detailed data-collection statistics are reported in Table 1.

3. Results and discussion

3.1. Multiple sequence alignment of DHARs, CLICs and GSTs

Sequence analysis was performed by comparing the sequences of DHARs, CLICs and GSTs using the *ClustalX* software (Thompson *et al.*, 1997; Fig. 1*a*). The human CLIC1 is the protein most similar to OsDHAR among the structurally determined proteins, with 32% sequence identity. Reduced CLIC1 is a monomer in solution and has a glutathione (GSH)-binding site surrounding the conserved Cys24 residue, which covalently binds to glutathione (Cromer *et al.*, 2002). Under oxidative conditions, CLIC1 undergoes an oligomeric state transition from a monomer to dimer as well as conformational changes, including intramolecular disulfide-bond formation. Disulfide-bond and dimer formation are essential for the development of integral membrane channels as well as the channel activity of CLIC1 (Littler *et al.*, 2004). The results of our sequence analysis revealed that OsDHAR also has a conserved catalytic cysteine residue and a GSH-

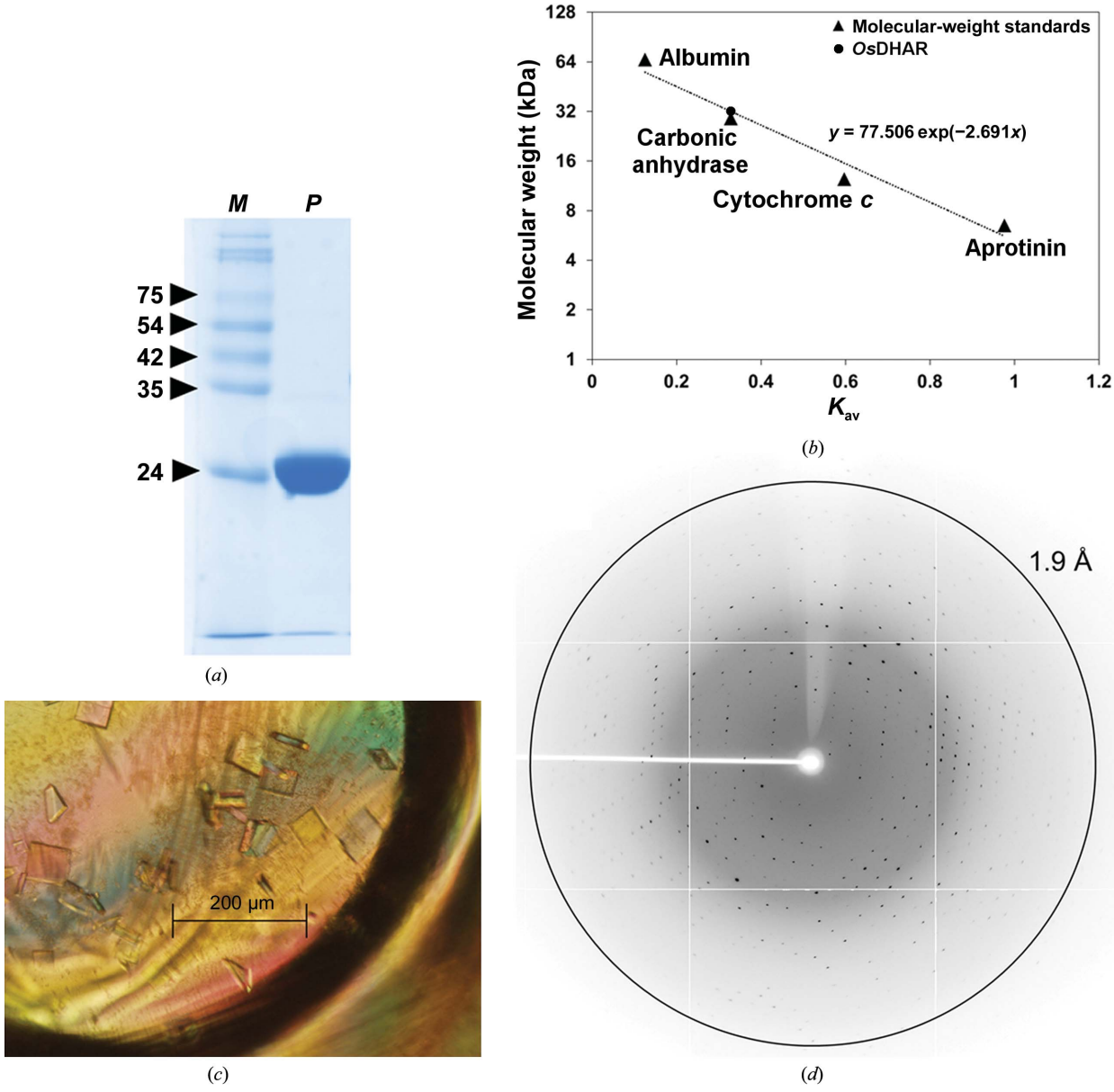

Figure 2
Purification, characterization and crystallographic studies of OsDHAR. (*a*) Purified OsDHAR protein (lane *P*) was loaded onto a 12% SDS–PAGE gel before the crystallization trials and the protein was visualized using Coomassie Blue stain. Lane *M* contains molecular-weight markers (labelled in kDa). (*b*) The molecular mass of OsDHAR was determined based on a standard curve obtained using a TSK gel G2000SWXL column. The elution volume indicated that OsDHAR was a monomer in solution with an apparent molecular weight of 31 kDa (V_e = 8.31 ml). The molecular-weight standards for gel filtration chromatography were albumin (66 kDa, V_e = 6.50 ml), carbonic anhydrase (29 kDa, V_e = 8.31 ml), cytochrome *c* (12.4 kDa, V_e = 10.70 ml) and aprotinin (6.5 kDa, V_e = 14.09 ml). The elution volume was used to calculate the partition coefficient $K_{av} = (V_e - V_o)/(V_t - V_o)$. (*c*) A crystal of OsDHAR was obtained using 0.15 *M* potassium bromide, 30%(*w*/*v*) PEG MME 2000 and its approximate dimensions were 0.1 × 0.1 × 0.05 mm. (*d*) X-ray diffraction image (1° oscillation range and 1.9 Å resolution limit) from an OsDHAR crystal.

binding site (Fig. 1*a*). However, the divergence of the α1–β2 region, which is a putative pore-forming helix in CLIC1 (residues 24-CPFSQRLFMVLWLKGVTFNVTTV-46), may reflect a different function of DHARs (Harrop *et al.*, 2001). We also included glutathione *S*-transferases (GSTs) in this sequence alignment because previous studies have shown that human GSTs belonging to the omega class (GSTO1-1 and GSTO2-2) have significant DHAR activity (Schmuck *et al.*, 2005; Zhou *et al.*, 2012). Omega-class GSTs have a conserved cysteine residue for GSH binding, whereas other classes of GSTs contain arginine, aspartate or serine residues in this corresponding location, which may explain why only the omega-class GSTs display DHAR activity (Fig. 1*b*).

3.2. Crystallographic studies on OsDHAR

OsDHAR consists of 213 amino-acid residues and has a theoretical isoelectric point of 5.81. The gene encoding OsDHAR was successfully cloned and the protein was overexpressed and purified. Approximately 22 mg OsDHAR was obtained per litre of culture, and its purity was estimated to be 96.6% based on densitometer (Gel Doc EZ imager with *Image Lab* software; Bio-Rad, Richmond, USA) scans of the SDS–PAGE gel (Fig. 2*a*). Moreover, the molecular weight of purified OsDHAR was analyzed by standard analytical SEC. OsDHAR was determined to have an apparent molecular weight of 31 kDa, indicating that the enzyme is a monomer in solution (Fig. 2*b*). Diffraction-quality crystals were obtained from an initial screening condition [0.15 *M* potassium bromide 30%(*w*/*v*) PEG MME 2000] by using the sitting-drop vapour-diffusion technique, and the drops consisted of 1 µl protein solution and 2 µl reservoir solution. The sitting drops were equilibrated against 0.3 ml reservoir solution at 298 K. The crystals diffracted to a resolution of 1.9 Å and a complete native data set was collected (Table 1). The OsDHAR crystal (Fig. 2*c*) belonged to the space group $P2_1$, with unit-cell parameters a = 47.03, b = 48.38, c = 51.83 Å, β = 107.41°. A diffraction image of the OsDHAR crystal is shown in Fig. 2(*d*). The Matthews coefficient (Matthews, 1968) was calculated to be 2.31 Å^3 Da^{-1} based on a monomer in the asymmetric unit, which corresponds to a solvent content of 46.88%. We have tried to use molecular-replacement (MR) methods for phase determination using *MOLREP* (Vagin & Teplyakov, 2010) and *Phaser* (McCoy *et al.*, 2007). However, MR failed to provide correct solutions for either the molecular orientation or molecular packing using the available structural homologues of human CLIC1 (PDB entry 1k0m, 32% sequence identity; Harrop *et al.*, 2001), CLIC4 (PDB entry 2d2z, 29% sequence identity; Li *et al.*, 2006), CLIC3 (PDB entry 3kjy, 24% sequence identity; Littler *et al.*, 2010) and CLIC2 (PDB entry 2r4v, 22% sequence identity; Cromer *et al.*, 2007). Next, we tried to identify an MR solution using a homology model of OsDHAR generated by the *SWISS-MODEL* server (Schwede *et al.*, 2003) using the coordinates of human CLIC1 as the template structure, and this protocol was successful whereas the original template failed. The rotation-function *Z*-score (RFZ), translation-function *Z*-score (TFZ) and the initial *R* value after a single round of refinement were 11.1, 7.3 and 39.5, respectively. The resulting PDB file was refined against the original data set using the macromolecular crystallographic refinement program *REFMAC*5 (Murshudov *et al.*, 2011), and reasonable $R_{\rm work}$ and $R_{\rm free}$ values of 16.3 and 20.6%, respectively, were obtained. After several rigid-body and restrained refinement steps, the resulting electron-density map was sufficient to build most residues. Additional studies on the structure refinement and model building of OsDHAR are currently under way. A more detailed structural comparison using fully refined structure models will contribute to a better understanding of the molecular mechanisms of this important enzyme.

We thank the staff at the X-ray core facility of the Korea Basic Science Institute (KBSI), Ochang, Korea and BL-5C of the Pohang Accelerator Laboratory, Pohang, Korea for their assistance with the data collection. This work was supported by the Antarctic organisms: Cold-Adaptation Mechanisms and its application grant (PE14070) funded by the Korea Polar Research Institute and a grant from the Next-Generation BioGreen 21 Program (No. PJ008115012014, Rural Development Administration, Republic of Korea).

References

Arrigoni, O. (1994). *J. Bioenerg. Biomembr.* **26**, 407–419.
Battye, T. G. G., Kontogiannis, L., Johnson, O., Powell, H. R. & Leslie, A. G. W. (2011). *Acta Cryst.* D**67**, 271–281.
Chen, Z. & Gallie, D. R. (2006). *Plant Physiol.* **142**, 775–787.
Chen, Z., Young, T. E., Ling, J., Chang, S.-C. & Gallie, D. R. (2003). *Proc. Natl Acad. Sci. USA*, **100**, 3525–3530.
Cromer, B. A., Gorman, M. A., Hansen, G., Adams, J. J., Coggan, M., Littler, D. R., Brown, L. J., Mazzanti, M., Breit, S. N., Curmi, P. M. G., Dulhunty, A. F., Board, P. G. & Parker, M. W. (2007). *J. Mol. Biol.* **374**, 719–731.
Cromer, B. A., Morton, C. J., Board, P. G. & Parker, M. W. (2002). *Eur. Biophys. J.* **31**, 356–364.
Gallie, D. R. (2013). *J. Exp. Bot.* **64**, 433–443.
Harrop, S. J. *et al.* (2001). *J. Biol. Chem.* **276**, 44993–45000.
Kelley, L. A. & Sternberg, M. J. (2009). *Nature Protoc.* **4**, 363–371.
Kim, Y.-S., Kim, I.-S., Bae, M.-J., Choe, Y. -H., Kim, Y.-H., Park, H.-M., Kang, H.-G. & Yoon, H.-S. (2013). *Planta*, **237**, 1613–1625.
Li, Y., Li, D., Zeng, Z. & Wang, D. (2006). *Biochem. Biophys. Res. Commun.* **343**, 1272–1278.
Littler, D. R., Brown, L. J., Breit, S. N., Perrakis, A. & Curmi, P. M. G. (2010). *Proteins*, **78**, 1594–1600.
Littler, D. R., Harrop, S. J., Fairlie, W. D., Brown, L. J., Pankhurst, G. J., Pankhurst, S., DeMaere, M. Z., Campbell, T. J., Bauskin, A. R., Tonini, R., Mazzanti, M., Breit, S. N. & Curmi, P. M. G. (2004). *J. Biol. Chem.* **279**, 9298–9305.
Matthews, B. W. (1968). *J. Mol. Biol.* **33**, 491–497.
McCoy, A. J., Grosse-Kunstleve, R. W., Adams, P. D., Winn, M. D., Storoni, L. C. & Read, R. J. (2007). *J. Appl. Cryst.* **40**, 658–674.
Murshudov, G. N., Skubák, P., Lebedev, A. A., Pannu, N. S., Steiner, R. A., Nicholls, R. A., Winn, M. D., Long, F. & Vagin, A. A. (2011). *Acta Cryst.* D**67**, 355–367.
Schmuck, E. M., Board, P. G., Whitbread, A. K., Tetlow, N., Cavanaugh, J. A., Blackburn, A. C. & Masoumi, A. (2005). *Pharmacogenet. Genomics*, **15**, 493–501.
Schwede, T., Kopp, J., Guex, N. & Peitsch, M. C. (2003). *Nucleic Acids Res.* **31**, 3381–3385.
Shin, S.-Y., Kim, M.-H., Kim, Y.-H., Park, H.-M. & Yoon, H.-S. (2013). *Mol. Cells*, **36**, 304–315.
Shin, S.-Y., Kim, I.-S., Kim, Y.-H., Park, H.-M., Lee, J.-Y., Kang, H.-G. & Yoon, H.-S. (2008). *Mol Cells*, **26**, 616–620.
Thompson, J. D., Gibson, T. J., Plewniak, F., Jeanmougin, F. & Higgins, D. G. (1997). *Nucleic Acids Res.* **25**, 4876–4882.
Tommasi, F., Paciolla, C., de Pinto, M. C. & De Gara, L. (2001). *J. Exp. Bot.* **52**, 1647–1654.
Tulk, B. M., Kapadia, S. & Edwards, J. C. (2002). *Am. J. Physiol. Cell Physiol.* **282**, C1103–C1112.
Ushimaru, T., Nakagawa, T., Fujioka, Y., Daicho, K., Naito, M., Yamauchi, Y., Nonaka, H., Amako, K., Yamawaki, K. & Murata, N. (2006). *J. Plant Physiol.* **163**, 1179–1184.
Vagin, A. & Teplyakov, A. (2010). *Acta Cryst.* D**66**, 22–25.
Warton, K., Tonini, R., Fairlie, W. D., Matthews, J. M., Valenzuela, S. M., Qiu, M. R., Wu, W. M., Pankhurst, S., Bauskin, A. R., Harrop, S. J., Campbell, T. J., Curmi, P. M. G., Breit, S. N. & Mazzanti, M. (2002). *J. Biol. Chem.* **277**, 26003–26011.
Yin, L., Wang, S., Eltayeb, A. E., Uddin, M. I., Yamamoto, Y., Tsuji, W., Takeuchi, Y. & Tanaka, K. (2010). *Planta*, **231**, 609–621.
Zhou, H., Brock, J., Liu, D., Board, P. G. & Oakley, A. J. (2012). *J. Mol. Biol.* **420**, 190–203.